



HAL
open science

Simulation and experimental investigation into Diffusion Absorption Cooling Machines for air-conditioning applications

U. Jakob, U. Eicker, D. Schneider, A.H. Taki, M.J. Cook

► **To cite this version:**

U. Jakob, U. Eicker, D. Schneider, A.H. Taki, M.J. Cook. Simulation and experimental investigation into Diffusion Absorption Cooling Machines for air-conditioning applications. Applied Thermal Engineering, 2008, 28 (10), pp.1138. 10.1016/j.applthermaleng.2007.08.007 . hal-00498961

HAL Id: hal-00498961

<https://hal.science/hal-00498961>

Submitted on 9 Jul 2010

HAL is a multi-disciplinary open access archive for the deposit and dissemination of scientific research documents, whether they are published or not. The documents may come from teaching and research institutions in France or abroad, or from public or private research centers.

L'archive ouverte pluridisciplinaire **HAL**, est destinée au dépôt et à la diffusion de documents scientifiques de niveau recherche, publiés ou non, émanant des établissements d'enseignement et de recherche français ou étrangers, des laboratoires publics ou privés.

Accepted Manuscript

Simulation and experimental investigation into Diffusion Absorption Cooling Machines for air-conditioning applications

U. Jakob, U. Eicker, D. Schneider, A.H. Taki, M.J. Cook

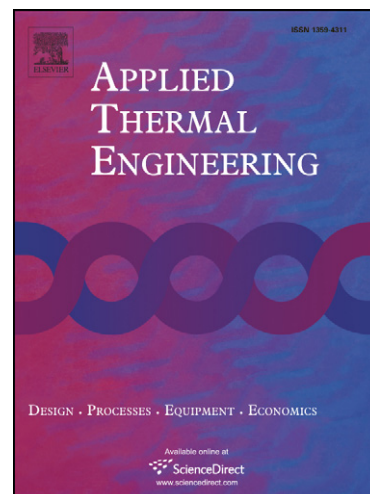
PII: S1359-4311(07)00284-0
DOI: [10.1016/j.applthermaleng.2007.08.007](https://doi.org/10.1016/j.applthermaleng.2007.08.007)
Reference: ATE 2249

To appear in: *Applied Thermal Engineering*

Received Date: 8 August 2006
Revised Date: 4 July 2007
Accepted Date: 16 August 2007

Please cite this article as: U. Jakob, U. Eicker, D. Schneider, A.H. Taki, M.J. Cook, Simulation and experimental investigation into Diffusion Absorption Cooling Machines for air-conditioning applications, *Applied Thermal Engineering* (2007), doi: [10.1016/j.applthermaleng.2007.08.007](https://doi.org/10.1016/j.applthermaleng.2007.08.007)

This is a PDF file of an unedited manuscript that has been accepted for publication. As a service to our customers we are providing this early version of the manuscript. The manuscript will undergo copyediting, typesetting, and review of the resulting proof before it is published in its final form. Please note that during the production process errors may be discovered which could affect the content, and all legal disclaimers that apply to the journal pertain.



Simulation and experimental investigation into Diffusion Absorption Cooling Machines for air-conditioning applications

U. Jakob^{1,*}, U. Eicker², D. Schneider², A. H. Taki³, M. J. Cook⁴

¹*SolarNext AG, Nordstrasse 10, D-83253 Rimsting, Germany*

²*Centre for Applied Research of Sustainable Energy Technology - zafh.net*

Stuttgart University of Applied Sciences, Schellingstrasse 24, D-70174 Stuttgart, Germany

³*Department of Product & Spatial Design (Incorporating Leicester School of Architecture)*

De Montfort University, The Gateway, Leicester LE1 9BH, U.K.

⁴*Institute of Energy & Sustainable Development (IESD), De Montfort University,*

Queens Building, The Gateway, Leicester LE1 9BH, U.K.

* Corresponding author. Tel.: +49-8051-6888-403; e-mail: uli.jakob@solarnext.de

Abstract

The paper presents the development, experimental analysis and simulation of a solar heat driven ammonia/water (NH₃/H₂O) Diffusion-Absorption Cooling Machine (DACM). The designed cooling capacity of the machine is 2.5 kW for air-conditioning applications. The indirectly heated generator with its bubble pump is the main new feature of this cooling machine and it showed good performance for all prototypes constructed. A major challenge of the technology is the constant total pressure level in all components, which makes condensate distribution into the evaporator vertical tubes with no distribution pressure extremely difficult. As a consequence, the first prototype

had problems in the auxiliary gas circuit, which only works with very low driving pressures and stops to work, when evaporation rates decay. In the second prototype, the auxiliary gas circulation was improved. However, the liquid condensate distribution into the evaporator remained problematically and the cooling power was limited to 1.6 kW maximum. Coaxial solution heat exchangers gave much better performance results than the initially chosen plate heat exchangers. In the third prototype the evaporator was optimised and the cooling capacity could be increased to 3 kW maximum. The maximum COP reached was 0.38. The Diffusion-Absorption Cycle was modelled using an expanded characteristic equation of sorption chillers. The simulation model showed good agreement with the measured data.

Keywords:

Diffusion absorption cooling machine; Ammonia/water; Bubble pump; Experimental results; Modelling; Simulation

1. Introduction

In recent years, the air conditioning market has been continuously expanding. In 2002 four percent growth was achieved, meaning nearly 44 million units sold annually. For the year 2008, market researchers expect 68.7 million units [1, 2]. The market is dominated by small split-units with a cooling capacity from 2 kW up to 4 kW. Due to the large number of manufactured units, these systems are produced and offered at very low prices; however, such systems increase environmental and sever grid overload problems as a result of using primary energy converted to electricity. Therefore, it is

important to search for alternative air-conditioning units that are driven by either waste heat or solar thermal energy as a renewable energy source.

State of the art are thermally driven Diffusion-Absorption Cooling Machines (DACM) with ammonia/water ($\text{NH}_3/\text{H}_2\text{O}$) and pressure compensated auxiliary gas circuit (helium or hydrogen) are commercially used only in a small power range up to 100 W. The priority operation criterion is the absolute noiselessness (hotel mini-bars) and the autonomous power supply (camping gas refrigerators). The well-known diffusion-absorption technique, which was developed in the 1920s by the Swedish engineers von Platen and Munters [3-5], is based on the principle of pressure equilibration between the high and low pressure sides of the unit through an inert auxiliary gas, such as helium or hydrogen. A further peculiarity of this type of absorption cooling machine is the use of a thermally driven gas bubble pump for the circulation of the solution cycle instead of a mechanical solution pump so that inside the cooling machine no mechanically moving parts are necessary. These small, simply constructed cooling machines, either driven by electrical heating cartridges or direct flame with a simple mechanical construction do not need conventional high-performance pumps or expansion valves, but show a very low coefficient of performance (COP) and therefore high energy consumption.

The gas, kerosene or electrically driven Diffusion-Absorption Refrigerators (DAR) were theoretically and experimentally investigated in numerous research projects concerning refrigeration applications [6-16]. Electrolux AB, Sweden (today Dometic AB) brought out the first refrigerator in 1925 [17]. Servel Inc. in Evansville, USA (today Robur SpA., Italy) produced refrigerators with small capacity under license starting in the

1930s and with their own design afterwards. Servel developed and produced a gas driven heat pump in 1937. This DAHP was water-cooled and the auxiliary gas used was hydrogen. The unit showed a COP of 0.19 with a cooling capacity of 1.75 kW and a heating capacity of 9.12 kW [18].

In the 1990s, these domestic DARs were modified and improved to be used as directly heated, gas driven Diffusion-Absorption Heat Pumps (DAHP). Values of Coefficient of Performance for heating applications (COP_{heat}) ranged from 1.2 to 1.35 for a heating capacity of 80 W to 205 W and with a cooling capacity between 25 W and 51 W [19]. Another group of researchers developed a directly gas heated DAHP with heating capacity between 3.0 kW and 3.5 kW at heating temperatures of 150°C and evaporator temperatures ranging from -15°C to +5°C [20,21]. The Coefficient of Performance for heating reached 1.5. The industrial conversion of this directly gas heated DAHP is carried out by BBT Thermotechnik GmbH, formerly Buderus Heiztechnik GmbH, in combination with a condensing boiler for a near-market unit, but is not yet commercially available. The output heating capacity of the DAHP is approximately 3.6 kW at a COP_{heat} of 1.5 [22]. Another industrial conversion of the DAHP has been done by Entex Energy Ltd. They realized DAHPs with 2.6 kW up to 8.0 kW heating capacity with a COP_{heat} of about 1.5. They also realized a directly gas driven DACM with 1.0 kW to 3.5 kW cooling capacity [23,24].

Up to now, some prototypes of small scale commercial absorption refrigerators with indirectly solar powered generators and hydrogen or helium as inert gas have also been experimentally and theoretically investigated. In these studies, COPs of 0.2 to 0.3 and

cooling capacities between 16 W and 62 W were reached at heating temperatures between 160°C and 230°C and evaporator temperatures of -6°C down to -18°C [25-28]. One research group used the DAHP of BBT Thermotechnik and modified it by substituting the direct gas fired generator by an indirectly heated device [29, 30]. The solar thermal heating capacity of 1.8 kW is provided by vacuum tube collectors. The cooling capacity is approximately 1 kW and the COP is 0.59 at a heating temperature of 175°C and an evaporator temperature of 2°C.

Reacting to the situation, that no suitable indirectly driven absorption cooling machines for air conditioning applications with low cooling power (1 kW to 5 kW) are available on the market, from 1998 to present the Stuttgart University of Applied Sciences and its sustainable energy research centre zafh.net developed and improved a solar heated ammonia/water DACM with a design cooling capacity of 2.5 kW and helium as pressure compensating inert gas [31-34]. This paper presents the detailed investigation of the performance potential as well as the experimental characterisation and optimisation of three prototypes with a newly developed indirectly heated generator/bubble pump. The performance of the prototypes are theoretically analysed and evaluated in the paper, using an expanded component model of the DACM process, which was developed based on the characteristic equations of sorption chillers.

2. Design of the prototypes

The core components of a DACM designed by the Stuttgart University of Applied Sciences are the generator, condenser, evaporator and absorber (see Figure 1). An indirectly powered generator / gas bubble pump is used for solution lifting. The solution

heat exchanger (SHX), the gas heat exchanger (GHX) in the auxiliary gas circuit and the dephlegmator for the condensation of the evaporated solvent are shell and tube, plate or coaxial heat exchangers, which are hermetically tight welded. The used working pair for the solution circulation is an ammonia/water mixture. Helium is used for the pressure compensation.

The prototypes of the solar driven DACMs are designed for the application area of air-conditioning as water chillers with an evaporator temperature of 6-12°C as well as for the operation of cooled ceilings with an evaporator temperature of 15-18°C. Table 1 summarises the technical design data of the developed prototypes.

3. Gas bubble pump performance

The directly driven bubble pump of DARS usually consists of a single lifting tube, where the heat input is restricted to a small heating zone by a heating cartridge or the flame of a gas burner with a high heat flux density. The indirectly driven DACM evaporator on the other hand consists of a bundle of tubes as bubble pump where the heating zone is spread and lower heat flux densities are reached. The developed bubble pumps are basically vertical shell-and-tube heat exchangers with the rich solution flow inside the tubes forming slug-flow at best and the heating medium flow on the shell side along baffled tube bundles.

The operation of the gas bubble pump is based on internal forced convection boiling, commonly referred to as two-phase flow, and is characterised by rapid changes from liquid to vapour in the flow direction. The indirectly heated vertical pipes of the bubble

pump are surrounded by a heat transfer medium, e.g. a water-glycol mixture or thermo oil. The ammonia/water solution rests in the bundle of pipes and when the tube walls are heated ammonia is expelled from the solution. Thereby, bubbles are formed at the inner surface of the tube walls under constant heat supply. This state of boiling is commonly called flow boiling. The internal flow boiling is distinguished into five two-phase flow regimes (bubbly flow, slug flow, annular flow, transition flow and mist flow) as shown in Figure 2. At low heat flux densities, slug flow is formed by an increasing number of germ cells. The bubbles form plugs which engage the whole circular tube section. This flow regime should be reached for operating the DACM generator in order to guarantee the solution lifting, solution circulation and the production of the necessary amount of ammonia for the cooling process.

For the characterisation of the gas bubble pump performance, five different bubble pump prototypes were constructed and compared. The performance values of the investigated range of generator heating temperatures and mass flow rates are presented in Table 2.

To measure the volume flow of the lifted weak solution, the so-called temperature flank method was used, as described in detail in [35]. The lifting ratio b is the ratio of lifted liquid volume \dot{V}_L to simultaneously expelled gas volume flow \dot{V}_V and is an important parameter to quantify the performance of the generator [36].

$$b = \frac{\dot{V}_L}{\dot{V}_V} \quad (1)$$

Another characteristic value of the generator is the specific solution circulation index f (see equation 2). This index is defined as the ratio of the mass flow rates of the rich

solution \dot{m}_{Sr} to the ammonia vapour \dot{m}_v expelled in the generator. Alternatively the ratio between the vapour X_{V1} and weak solution concentration X_{Sw} to the degassing width E , defining the difference between weak and rich solution concentration X_{Sw} and X_{Sr} , can be used to determine the specific solution circulation index f .

$$f = \frac{\dot{m}_{Sr}}{\dot{m}_v} = \frac{X_{V1} - X_{Sw}}{X_{Sr} - X_{Sw}} \quad (2)$$

The solution concentrations used varied between 24 and 34% for the weak solution X_{Sw} and 30 to 45% for the rich solution X_{Sr} . With decreasing degassing width the specific solution circulation increased from 4 (13-14% degassing) up to 15 (for 4% degassing width).

The maximum volume flow of the lifted weak solution was 53 l h^{-1} at a vapour volume flow of 12.2 l h^{-1} , resulting in a lifting ratio of 4.3 at an external generator inlet temperature of 165°C . Figure 3 shows three plots of measured liquid volume flow, the calculated vapour volume flow and the lifting ratio of the first prototype and generator No.3. Up to a temperature level of 165°C , the volume flow of the vapour increased continuously with generator temperature. Above 165°C the slug flow collapsed and converted to annular flow, while nucleate boiling changed to film boiling. Therefore, at heating temperatures above 165°C , more vapour is generated but the solution lifting decreases.

Converted to mass flows, the lifted weak solution volume flow shows a maximum of 42.0 kg h^{-1} and a vapour mass flow of 6.0 kg h^{-1} resulting in a specific solution circulation index f of 8.0 at an external generator inlet temperature of 165°C . The design

value for the mass flow of the weak solution for a 2.5 kW evaporator cooling capacity is higher at 50 kg h^{-1} and the ammonia vapour mass flow should be 8 kg h^{-1} .

The developed bubble pumps worked in a wide range of temperatures as well as external heating volume flow rates. Figure 4 shows a comparison of COPs and evaporator cooling capacities at a high and a low generator external heating volume flow of the DACM No.2 with coaxial SHX. The cooling capacities were up to 30% higher when the external heating volume flow rates were increased from 15 liters per minute to 34 liters per minute. Similar measurements were later done on the third prototype. Again, at constant generator input power, the cooling power increased with increasing mass flow. Higher external heat transfer coefficients reduce the temperature difference between the external mass flow and the tube surface, thus producing higher wall temperatures and more ammonia production.

To dimension the tube diameters for the generator, equations derived by Chisholm, Taitel and others were used [37]. To maintain slug flow the maximum value of the tube diameter increases with increasing surface tension and decreases with liquid density. The minimum tube diameter increases with the desired vapour volume flow and decreases with increasing surface tension. For the operating conditions chosen, slug flow was calculated for tubes with an inner diameter ranging from 5 mm to 41 mm.

The required minimum height difference of the bubble pump between the rich solution level in the reservoir and the level of the boiling zone was calculated using equations derived by Narayankhedkar and others and Chen [38, 39]. This correlation is based on the assumptions that all bubbles are formed at the bottom of the minimum height difference (see Figure 5), so that there is no relative velocity between the weak solution

and the refrigerant vapour bubbles in the tube and that friction losses and vapour pressure of the absorbent water are negligible.

For a relative molecular mass of the refrigerant ammonia of 17 kg kmol^{-1} and the given data in Table 3 the calculated minimum height difference is 0.12 m for DACM No.1 and 0.03 m for DACM No.2.

4. Further experimental results from DACM No.1

The first pilot plant was put into operation in November 2000. A series of measurements were taken at generator heating inlet temperatures of 150°C to 175°C and evaporator temperatures between 25°C and 0°C . The measurements were taken with and without a dephlegmator. A maximum COP of 0.2 could be achieved and the evaporator cooling capacity of the pilot plant showed values from 0.5 kW to 1.5 kW. The first prototype could not be continuously operated. The evaporator capacity decreased with time as shown in Figure 6, as the auxiliary gas starts to get saturated with ammonia caused by an insufficient auxiliary gas circulation. This could not be attributed to excessive pressure drops in the auxiliary gas circuit. At auxiliary gas volume flows below $4 \text{ m}^3 \text{ h}^{-1}$, the pressure drop calculated and measured after deconstruction of the prototype was 1 Pa only and the driving force calculated from the density difference between ammonia rich auxiliary gas and weak gas after the absorber is 15 Pa for 5°C evaporation temperature and a height difference of 1 m between evaporator and absorber. The saturation can thus only be attributed to low rates of evaporation, which could be caused by very uneven distribution of liquid ammonia into the tubes of the falling film evaporator.

Due to the low heat recovery factors Φ_{Sr} and Φ_{Sw} of the tubular SHX of 39.6% and 51.1% for DACM No.1 (the low and high values correspond to the rich and weak solution sides with different mass flow rates) the measured generator heating capacities were high between 10.0 kW and 13.5 kW at an operation pressure of 20×10^5 Pa and the COPs accordingly low (around 0.1).

5. Further experimental results from DACM No.2

A second more compact prototype was built based on the experiences and results from the first, using partly standard commercial components such as nickel soldered plate heat exchangers and a coaxial heat exchanger for the condenser and the solution heat exchanger, respectively. For this prototype, a further indirectly heated bubble pump was developed and the auxiliary gas circuit was constructively reworked. These changes resulted in weight reduction down to 290 kg and height reduction down to 2.40 m which are important factors for a more marketable unit. The second prototype was put into operation in July of 2003 and run till July of 2005.

Measuring results with stationary temperature, pressure and capacity levels were done with variation of the heating temperatures, the cooling water temperatures and the cold brine temperatures. The heating temperature range of the generator was reduced from 150°C to 175°C of the first pilot plant to 110°C to 140°C for the second pilot plant. This is due to the decreased lifting height of the bubble pump by half and an increased heat transfer surface. The continuous evaporator cooling capacities at an operation pressure of 18×10^5 Pa were around 0.5 kW with COPs between 0.1 and 0.2. The maximum cooling capacity reached was 0.8 kW.

6. Solution heat exchange behaviour

The plate SHX was replaced by a coaxial SHX due to very low heat recovery factors of 11.4% and 31.2% for the rich and weak solution sides respectively. At such low mass flow rates, the flow conditions in the plate heat exchanger are laminar and the delay time of the liquid is low for the small volumes. The coaxial solution heat exchanger on the other hand has a large volume with a long flow section, so that the liquid stays longer in the tubes and the heat recovery factors improved to 76% and 92%. The COP was now between 0.2 to 0.3 and continuous evaporator cooling performance of 0.5 kW to 1.5 kW was reached (see Figure 7) at a pressure of 20×10^5 Pa. A maximum cooling capacity of 2 kW could be achieved, if the evaporator inlet temperature was set to values of around 25°C, indicating insufficient evaporation inside the evaporator tubes.

7. Pressure dependence

Further measurements were carried out at a lower operating pressure of 12×10^5 Pa and serial absorber-condenser cooling water inlet temperatures of 27°C and outlet up to 33°C (see Figure 8). Many long term measurements of up to 11 days were carried out without shutting down the machine. The performance was improved to a COP of 0.3 to 0.45 and a continuous evaporator cooling performance up to 1.6 kW at evaporator outlet temperatures for air-conditioning and cooled ceilings between 22°C and 15°C. The lowest logged external evaporator outlet temperature was -5°C at an operation pressure of 8.5×10^5 Pa and a generator heating inlet temperature of 145°C.

The performance improvements can be attributed to the lower total pressure of the system, which improves both the vapour bubble formation process inside the generator

and the diffusion mass flow rates in the evaporator. The COP curve decreasing with generator temperature indicates that the available amount of ammonia condensate is not completely evaporated inside the vertical falling film evaporator. A comparison of the resulting theoretically possible and the measured cooling capacity of the existing falling film evaporator shows that above a generator heating inlet temperature of 125°C the falling film evaporator was not able to convert the amount of liquid ammonia into cooling capacity.

8. Evaporator performance

From the measured liquid ammonia mass flow, a theoretically possible evaporator cooling capacity was determined between 0.6 and 2.7 kW for heating temperatures between 115 and 155°C. The measured cooling capacities were only between 0.6 kW to 1.5 kW. The falling film evaporator could not evaporate all of the available liquid ammonia into the helium gas atmosphere, not even with high external evaporator inlet temperatures of around 25°C. Therefore, the falling film evaporator needs to be rebuilt with either more or longer evaporation tubes so that a larger heat transfer surface is created, which would lead to a smaller film thickness and therefore, a longer delay time. Also the issue of liquid distribution into the evaporator tubes plays an important role for the evaporator performance. At the given very low condensate flow rates it is extremely difficult to obtain an even distribution of liquid into all tubes of the evaporator. Experiments with metal wicks and annular capillary systems are currently carried out to improve the liquid distribution.

9. Experimental results from DACM No.3

The experimental investigations of the third DACM with marketable dimensions are focused on the combined evaporator-GHX-absorber unit and the new generator (Figure 9). The heating temperature range of the generator was reduced from 150°C to 175°C of the first prototype to 110°C to 155°C for the second prototype and now to 100°C to 150°C of the third prototype. The experimental results show evaporator cooling capacities from 0.7 kW up to 3.0 kW and COPs between 0.12 and 0.38. The obtained evaporator temperatures are 12/6°C and 18/15°C (Figure 10). The lowest logged external evaporator outlet temperature was -15°C at a generator heating inlet temperature of 135°C.

10. Modelling and simulation

The Diffusion-Absorption Cycle has been modelled starting from the constant characteristic equation of sorption chillers developed by Ziegler [40], which is an exact solution of the internal mass and energy balances of each component as well as the heat transfer between external and internal temperature levels for only one given design point. These equations are used in a simple linear equation for different boundary conditions. For larger deviations from design conditions or for absorption chillers with thermally driven bubble pumps, one single equation does not represent the chiller performance accurately [41].

Several problems are associated with a steady-state, single characteristic equation that calculates all internal enthalpies only for the design conditions. If a thermally driven bubble pump is used as in a DACM, the rich solution mass flow rate strongly depends on the generator heating temperature and external mass flow rate of the heating circuit. Also, if the external temperature levels differ significantly from design conditions, the

internal temperature levels change and consequently, so do the enthalpies. Therefore, an expanded characteristic equation based on changing internal enthalpies (so-called variable enthalpy) and changing rich solution mass flow rates for each time step was carried out for the DACM [37].

The expanded characteristic equation is set up for the working pair $\text{NH}_3/\text{H}_2\text{O}$. Additional components such as the dephlegmator, the auxiliary gas circuit (auxiliary gas cooling losses) or GHX and the bubble pump with the variable mass flow rates corresponding to external heating temperature based on the characteristics of the bubble pump are included.

The expanded model was implemented in the simulation environment INSEL [42] and validated by experimental data of the optimised prototype, DACM No.2 (see Figure 11). The results of the simulation runs of the DACM showed that the performance of the DACM, with variable enthalpy, describes the experimental data of the measured performance with a deviation of less than 6.5 % for the COP.

Furthermore a parameter study was carried out to determine strategies to improve the performance of the DACM at different evaporator inlet and cooling water temperatures in combination with evaporator surface wetting factors and gas heat exchanger (GHX) recovery factors [37]. For the DACM No.2 with coaxial SHX, a surface wetting factor ε_w of 1.0 and a GHX efficiency Φ_{GHX} of 0.3, the design cooling capacity of 2.5 kW could be reached for evaporator inlet temperatures of 12°C and 24°C and corresponding generator heating inlet temperatures of 162°C and 123°C. The corresponding COPs were 0.38 and 0.85. The very high COP of 0.85 shows the importance of full wetting of

the tubes combined with high evaporator temperatures for the highest evaporation rates. Also, a better performance of the absorber at low absorber cooling inlet temperature increases the evaporator cooling capacity due to higher driving pressure difference. Figure 12 presents the performance at different GHX heat recovery factors for an evaporator inlet temperature of 12°C and a constant generator temperature of 130°C. If the heat recovery factor increases from the measured value of 0.30 to 0.60, both cooling capacity and COP increase by a factor 1.1 to 1.2. To achieve this improvement it is necessary to optimise the heat transfer inside the GHX using constructive steps to reach higher heat recovery factors.

The results of the simulation runs of the DACM showed a strong influence of the surface wetting factor ε_w as well as the heat recovery factor Φ_{GHX} of the gas heat exchanger of the falling film evaporator on the evaporator cooling capacity. Other important influences on the performance of the DACM are the heat losses Q_{Ax} and Q_{Gx} as well as $\Delta\Delta t_{min,E}$, which depend on the rich solution mass flow m_{Sr} , i.e. on the bubble pump performance.

11. Conclusions

In this work, a Diffusion Absorption Cooling Machine of 2.5 kW design cooling capacity was developed, experimentally characterised and modelled using an expanded version of the characteristic equation. The indirectly heated generator with a bubble pump for liquid solution transport showed good performance and the required flow rates for both solution and vapour could be obtained using a shell and tube construction. The main challenge of the machine development was the low performance of the auxiliary

gas circuit on the evaporator/absorber side. The distribution of small amounts of condensed ammonia under no extra pressure into the numerous evaporator tubes proved difficult and various constructive solutions for liquid distribution were tested. Best results were obtained for capillary ring tubes inserted into the evaporation tubes.

Several heat exchanger types were analysed in the solution circuit and the condenser. Whereas plate heat exchangers performed well for the condenser, very low heat recovery factors were measured in the solution circuit. This could be attributed to laminar flow conditions and short liquid delay times in the heat exchangers. Much better results were obtained for coaxial heat exchangers.

The third prototype, which has now marketable dimensions, reached cooling capacities between 0.7 kW and 3.0 kW at evaporator temperatures of 12/6°C and 18/15°C with COPs from 0.12 to 0.38 (Table 4).

An expanded, steady-state model of the DACM based on the characteristic equation of sorption chillers showed a good accordance of the compared experimental and simulated data. Efficient evaporation with high surface wetting factors is essential for high performance.

Acknowledgements

This work was partly funded within a Craft research project by the European Commission in the framework of the Non Nuclear Energy Programme JOULE III, contract number JOE3-CT98-7045. The work of the modelling and simulation is carried out by the Centre for Applied Research of Sustainable Energy Technology - zafh.net which is funded by the Landesstiftung Baden-Württemberg. The current development of

the DACM is supported by the German Federal Ministry of Economy and Work (BMWA), grant number 0327351A.

References

- [1] JRAIA, Estimates of World Demand for Air Conditioners (2000-2008), The Japan Refrigeration and Air Conditioning Industry Association, 2006. URL: www.jraia.or.jp/english/.
- [2] Der Klimamacher, Der Welt- und Europamarkt für Raumklimageräte, CCI.Print - Der Klimamacher Wissen+Praxis 37 (3) (2003).
- [3] C.G. Munters, Entwicklung des Elektrolux-Kühlapparates, Zeitschrift für die gesamte Kälte-Industrie 39 (11) (1932) 197-200 and 39 (12) 216-220.
- [4] K.E. Herold, R. Rademacher, S.A. Klein, Absorption Chillers and Heat Pumps (1st edit.), Boca Raton: CRC Press, USA, 235-242, 1996. ISBN 0-8493-9427-9.
- [5] F.G. Watts, C.K. Gulland, Triple-fluid vapour-absorption refrigerators, The J. of Refrig. July and August (1958) 107-115.
- [6] H. Stierlin, Neue Möglichkeiten für den Absorptions-Kühlschrank (New chances for the absorption refrigerator), Kältetechnik 9 (1964) 264-270.
- [7] M. Bäckström, E. Emblik, Kältetechnik (3rd edit.), Karlsruhe: Verlag G. Braun, Germany, 650-653, 1965.
- [8] B. Reistad, Thermal conditions in heat driven refrigerating units for domestic use, Kylteknisk tidskrift 27 (3) (1968) 43-51.
- [9] K.G. Narayankhedkar, M.P. Maiya, Investigations on triple fluid vapour absorption refrigerator, Int. J. Refrigeration 8 (11) (1985) 335-342.

- [10] D.A. Kouremenos, A. Stegou-Sagia, K.A. Antonopoulos, Three-dimensional evaporation process in aqua-ammonia absorption refrigerators using helium as inert gas, *Int. J. Refrigeration* 17 (1) (1994) 58-67.
- [11] K.J. Kim, Z. Shi, J. Chen, K.E. Herold, Hotel room air conditioner design based on the Diffusion-Absorption cycle, *ASHRAE Technical Data Bulletin* 11 (2) (1995) 47-58.
- [12] J. Chen, K.J. Kim, K.E. Herold, Performance enhancement of a diffusion-absorption refrigerator, *Int. J. Refrigeration* 19 (3) (1996) 208-218.
- [13] G.F. Smirnov, M.A. Bukraba, T. Fattuh, B. Nabulsi, Domestic refrigerators with absorption-diffusion units and heat-transfer panels, *Int. J. Refrigeration* 19 (8) (1996) 517-521.
- [14] G. Vicatos, Experimental investigation on a three-fluid absorption refrigeration machine, *Proceedings of the Institution of Mechanical Engineers (Part E)* 214 (3) (2000) 157-172.
- [15] P. Srihirin, S. Aphornratana, Investigation of a diffusion absorption refrigerator, *Applied Thermal Engineering* 22 (11) (2002) 1181-1193.
- [16] T. Al-Shemmeri, Y. Wang, Theoretical investigation and parameter study of a diffusion absorption refrigeration system, In: *Proceedings of the 21st IIR International Congress of Refrigeration*, 2003 August 17-22; Washington D.C., USA. Paris: International Institute of Refrigeration (IIR), 2002, ISBN 2-913149-32-4.
- [17] W. Niebergall, Sorptions-Kältemaschinen, in: R. Plank (eds.), *Handbuch der Kältetechnik* (reprint 1st edit.), Berlin: Springer-Verlag, Germany, Vol. 7, 105-114, 1981.

- [18] R. Plank, J. Kuprianoff, Die Kleinkältemaschine (2nd edit) Berlin: Springer-Verlag, Germany, 360-397, 1960.
- [19] K.E. Herold, Diffusion-Absorption Heat Pump, Final Report for Gas Research Institute, GRI-96/0271, Gas Research Institute, USA, 1996.
- [20] W. Schirp, Gasbeheizte Diffusions-Absorptions-Wärmepumpe (DAWP) für Wohnraumbeheizung, Brauchwassererwärmung und Wohnraumkühlung, *Klima-Kälte-Heizung* 18 (3) (1990) 113-118.
- [21] H.C. Stierlin, J.R. Ferguson, Diffusion Absorption Heat Pump (DAHP), *ASHRAE Transactions (AT-90-27-4)* 96 (1990) 1499-1505.
- [22] C. Schwarz, D. Lotz, Gas-Wärmepumpen - Absorber: Einsatz im Ein- und Zweifamilienwohnhaus, in: *Proceedings of the Fachtagung Heizen - Kühlen - Klimatisieren mit Gas-Wärmepumpen und -Kälteanlagen*, 2001 November 14; Fulda, Germany. Kaiserslautern: ASUE, 2001, 35-43. URL: www.asue.de.
- [23] Entex, Gaswärmepumpe aus der Schweiz, *Sonne Wind & Wärme* 28 (10) (2004) 34.
- [24] Entex, Company internet documents, Entex Energy Ltd, Eggenwil, Switzerland, 2005. URL: www.entex-energy.ch.
- [25] C. Keizer, Absorption refrigeration machine driven by solar heat, in: *Proceedings of the 15th IIR International Congress of Refrigeration*, 1979; Venetian, Italy. Paris: International Institute of Refrigeration (IIR), 1979, 861-868.
- [26] P. Bourseau, J.C. Mora, R. Bugarel, Coupling of absorption-diffusion refrigeration machine and a solar flat-plate collector, *Int. J. Refrigeration* 10 (4) (1987) 209-216.

- [27] F. Gutiérrez, Behaviour of a household absorption-diffusion refrigerator adapted to autonomous solar operation, *Solar Energy* 40 (1) (1988) 17-23.
- [28] S. Ajib, P. Schultheis, Untersuchungsergebnisse einer solarthermisch betriebenen Absorptionskälteanlage, *TAB Technik am Bau* 29 (2) (1998) 49-54.
- [29] R. Braun, R. Hess, Solar Cooling, in: *Proceedings of the 7th World Renewable Energy Congress*, 2002 July 1-5; Cologne, Germany. Reading: World Renewable Energy Network (WREN), 2002, ISBN: 0-08-044079-7.
- [30] W. Stürzebecher, R. Braun, E. Garbett, M. Denman, Solar driven sorption refrigeration systems for cold storage depots, in: *Proceedings of the 3rd International Conference on Heat Powered Cycles (HPC 2004)*, 2004 October 11-13; Larnaca, Cyprus. London: South Bank University, 2004, paper no. 2117.
- [31] U. Jakob, U. Eicker, Solar Cooling with Diffusion Absorption Principle, in: *Proceedings of the 7th World Renewable Energy Congress*, 2002 July 1-5; Cologne, Germany. Reading: World Renewable Energy Network (WREN), 2002, ISBN: 0-08-044079-7.
- [32] U. Jakob, U. Eicker, A.H. Taki, M.J. Cook, Development of an optimised solar driven Diffusion-Absorption Cooling Machine, in: *Proceedings of the ISES Solar World Congress*, 2003 June 16-19; Göteborg, Sweden. Freiburg: International Solar Energy Society (ISES), 2003, ISBN: 91-631-4740-8.
- [33] U. Jakob, U. Eicker, D. Schneider, M.J. Cook, A.H. Taki, Neue Ergebnisse einer solar thermisch betriebenen Diffusions-Absorptionskältemaschine kleiner Leistung, in: *Proceedings of the 14th Symposium Thermische Solarenergie*, 2004 May 12-14; Staffelstein, Germany. Regensburg: Ostbayerisches Technologie-Transfer-Institut e.V. (OTTI), 2004, 482-487, ISBN 3-934681-33-6.

- [34] U. Jakob, U. Eicker, A.H. Taki, M.J. Cook, Development of a solar powered Diffusion Absorption Cooling Machine, in: Proceedings of the 1st International Conference Solar Air-Conditioning, 2005 October 6-7; Staffelstein, Germany. Regensburg: Ostbayerisches Technologie-Transfer-Institut e.V. (OTTI), 2005, 111-115, ISBN 3-934681-41-7.
- [35] A. Biesinger, Untersuchungen an einem indirekt beheizten Austreiber einer Diffusions-Absorptionskältemaschine (DAKM), Diploma Thesis, Fachhochschule Stuttgart-Hochschule für Technik, 2002.
- [36] A.G. Cattaneo, Über die Förderung von Flüssigkeiten mittels der eigenen Dämpfe – Thermosyphon-Prinzip, Zeitschrift für die gesamte Kälteindustrie 42 (1) (1935) 2-8, 42 (2) (1935) 27-32 and 42 (3) (1935) 48-53.
- [37] U. Jakob, Investigations into Solar Powered Diffusion-Absorption Cooling Machines, PhD Thesis, De Montfort University Leicester, 2005.
- [38] K.G. Narayankhedkar, M.P. Maiya, Investigations on triple fluid vapour absorption refrigerator, Int. J. Refrigeration 8 (11) (1985) 335-342.
- [39] J. Chen, Further Development of the Diffusion-Absorption Refrigerator, PhD Thesis, University of Maryland, 1995.
- [40] F. Ziegler, Sorptionswärmepumpen, Forschungsberichte des Deutschen Kälte- und Klimatechnischen Vereins No. 57, Stuttgart: DKV, 1998, ISBN 3-932715-60-8.
- [41] J. Albers, F. Ziegler, Analysis of the part load behaviour of sorption chillers with thermally driven solution pump, in: Proceedings of the 21st IIR International Congress of Refrigeration, 2003 August 17-22; Washington D.C., USA. Paris: International Institute of Refrigeration (IIR), 2002, ISBN 2-913149-32-4.

- [42] J. Schumacher, Digitale Simulation regenerativer elektrischer Energieversorgungssysteme, Dissertation, Universität Oldenburg, 1991. URL: www.insel.eu

ACCEPTED MANUSCRIPT

Nomenclature

A_E	specific absorber enthalpy coefficient
$A_{E,aux}$	additional specific absorber enthalpy coefficient
B	Dühring constant
b	lifting ratio
C_E	specific condenser enthalpy coefficient
COP	coefficient of performance
COP_{heat}	coefficient of performance for heating applications
$c_{L,NH_3/H_2O}$	specific heat capacity of liquid ammonia ($\text{kJ kg}^{-1} \text{K}^{-1}$)
c_{V,NH_3}	specific heat capacity of ammonia vapour ($\text{kJ kg}^{-1} \text{K}^{-1}$)
D	inner tube diameter (mm)
E	degassing width
f	specific solution circulation index
G_E	specific generator enthalpy coefficient
$G_{E,deph}$	additional specific dephlegmator enthalpy coefficient
h_L	liquid enthalpy of condensed ammonia/water vapour (kJ kg^{-1})
h_V	vapour enthalpy of ammonia/water vapour (kJ kg^{-1})
m_{Sr}	mass flow rate of rich ammonia/water solution (kg s^{-1})
m_{Sw}	mass flow rate of weak ammonia/water solution (kg s^{-1})
m_Y	mass flow rate of ammonia(/water) vapour (kg s^{-1})
p	total pressure (Pa)
p_{NH_3}	ammonia partial pressure (Pa)
Q_A	absorber cooling capacity (kW)
Q_{AUX}	auxiliary gas circulation cooling loss capacity (kW)

Q_{Ax}	solution heat loss (kW)
Q_C	condenser cooling capacity (kW)
Q_{Deph}	dephlegmator cooling capacity (kW)
Q_{Gx}	solution heat loss (kW)
Q_H	generator heating capacity (kW)
Q_O	evaporator cooling capacity (kW)
s_E	slope of the characteristic equation (kW K ⁻¹)
T	temperature (°C)
T	mean internal temperature (°C)
$T_{C,s}$	condensation temperature (°C)
T_G	mean internal generator temperature (°C)
$T_{H,in}$	external generator inlet temperature (°C)
T_{LC}	condenser liquid outlet temperature (°C)
T_{SwG}	generator outlet temperature of the weak solution (°C)
T_{VC}	condenser vapour inlet temperature (°C)
t	mean external temperature (°C)
$\Delta\Delta t$	characteristic double temperature difference (K)
$\Delta\Delta t_{min,E}$	intersection of the characteristic equation (K)
UA	heat transfer coefficient (kW K ⁻¹)
V_L	lifted volume flow (l/h)
V_V	expelled gas volume flow (l/h)
X_{Sr}	ammonia mass concentration of rich ammonia/water solution
X_{Sw}	ammonia mass concentration of weak ammonia/water solution
X_V	ammonia vapour mass concentration, vapour purity

X_{V1} non-rectified ammonia/water vapour mass concentration

Greek letters

ε_w surface wetting factor

Φ_{GHX} heat recovery rate of the gas heat exchanger

Φ_{Sr} heat recovery factor referred to rich solution side

Φ_{Sw} heat recovery factor referred to weak solution side

Abbreviations

ACM Absorption Cooling Machine

DACM Diffusion-Absorption Cooling Machine

DAHP Diffusion-Absorption Heat Pump

DAR Diffusion-Absorption Refrigerator

GHX gas heat exchanger

NH_3/H_2O ammonia/water

SHX solution heat exchanger

Subscripts

A, a absorber

C, c condenser

D, d dephlegmator

E, e, O evaporator

G, g, H generator

List of Figures

Fig. 1: Principle of the DACM process.

Fig. 2: Flow regimes and heat transfer coefficients of two-phase vertical flows in a bubble pump [37].

Fig. 3: Liquid and vapour volume flows and lifting ratios of generator No.3 of DACM No.1 as a function of external generator inlet temperature.

Fig. 4: Influence of external volume flow in the generator of the DACM No.2 on cooling capacity and COP as a function of external generator inlet temperature (September/October 2004).

Fig. 5: Bubble pump configuration.

Fig. 6: Operating performance of the DACM No.1 as a function of time with increasing saturation of the auxiliary gas (February 2002).

Fig. 7: COP and heating and cooling capacity of the DACM No.2 (coaxial SHX) ranges as a function of generator heating water inlet temperatures (April 2004). The total pressure was 20×10^5 Pa, cooling water inlet to the absorber was 20°C , to the condenser 35°C and the evaporator inlet temperature was 25°C .

Fig. 8: COP and heating and cooling capacity of the DACM No.2 with coaxial SHX at a lower total pressure of 12×10^5 Pa as a function of generator heating water inlet temperatures (September 2004).

Fig. 9: Third prototype of the Diffusions Absorption Cooling Machine.

Fig. 10: COP and cooling capacity of the DACM No.3 for different evaporator temperatures as a function of generator inlet temperature (May 2006). The total pressure was 11×10^5 Pa, cooling water inlet to the absorber was 28°C and to the condenser 25°C .

Fig. 11: Measured and simulated values of the DACM No.2 as a function of generator inlet temperature (design $t_e=22.5^\circ\text{C}$ at 1.3 kW cooling capacity as well as $t_g=140^\circ\text{C}$, $t_a=29^\circ\text{C}$ and $t_c=32^\circ\text{C}$ with SHX and GHX efficiency of 0.76 and 0.30, respectively).

Fig. 12: Effect of different GHX heat recovery factors on the performance of the DACM No.2 with coaxial SHX at an evaporator inlet temperature of 12°C and fixed generator heating inlet temperature of 130°C as a function of varied surface wetting factors.

List of Tables

Table 1: Design conditions for Diffusion Absorption Cooling Machine.

Table 2: Pressure levels, concentration ranges and specific solution circulation in the generator No.3 and No.5 of DACM prototypes No.1 and No.2.

Table 3: Boundary conditions and minimum height difference between the top level of the reservoir and the heating zone of the bubble pump.

Table 4: Summary of DACM prototype development.

ACCEPTED MANUSCRIPT

Tables

Table 1

COP (coefficient of performance, ratio of cooling output to driving heat input)		0.48
generator	heating capacity Q_H	5.2 kW
	heating water in/out	130/120°C
dephlegmator	cooling capacity Q_{Deph}	0.9 kW
	cooling water in/out	34/38°C
condenser	cooling capacity Q_C	2.8 kW
	cooling water in/out	31/34°C
evaporator	refrigerating capacity Q_O	2.5 kW
	cold brine in/out	12/6°C
absorber	cooling capacity Q_A	4.0 kW
	cooling water in/out	27/31°C

Table 2

characteristic values	generator No.3		generator No.5	
total pressure p [10^5 Pa]	20	18	20	12
NH ₃ initial concentration [%]	38	30	40	37
rich NH ₃ -solution conc. X_{Sr} [%]	45–42	30	40	37
weak NH ₃ -solution conc. X_{Sw} [%]	31–34	24–26	31–33	24–29
degassing width E [%]	14–8	6–4	9–7	13–8
vapour concentration X_{Vl} [%]	88–91	82–85	89–91	84–89
specific solution circulation f [-]	4–7	11–15	6.5–8.5	4.5–7.5

Table 3

	DACM No.1	DACM No.2
generator mean boiling temperature T_b [°C]	130	110
NH3 rich/weak mass concentration X_{Sr} / X_{Sw} [-]	0.42 / 0.34	0.37 / 0.27
rich/weak solution density ρ_{Sr} / ρ_{Sw} [kg m ⁻³]	742 / 783	789 / 837
total pressure p [10 ⁵ Pa]	20	12
lifting height Δh [m]	1.00	0.50
minimum height difference Y [m]	0.12	0.03

Table 4

prototypes	DACM No.1	DACM No.2 plate SHX	DACM No.2 coaxial SHX	DACM No.3
evaporator cooling capacity Q_o [kW]	0.5 – 1.5	0.5 – 0.8	0.5 – 2.0	0.7 – 3.0
COP [-]	0.10 – 0.20	0.10 – 0.15	0.20 – 0.45	0.12 – 0.38
weight [kg]	800	290	240	240
area [m ²]	1.5 x 1.5	0.8 x 0.8	0.8 x 0.8	0.6 x 0.6
height [m]	3.7	2.4	2.4	2.2
results	helium atmosphere saturated, low COP and high weight	heat recovery factor SHX < 15%	improvement of COP and cooling capacity	cooling capacity reached, heating temperatures of 100-150°C

Figure 1

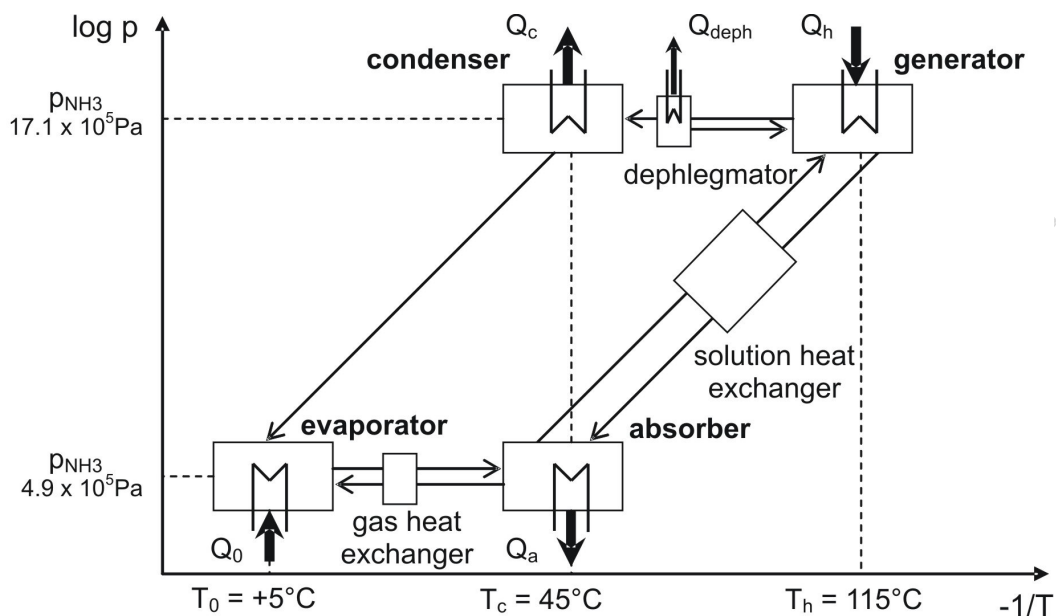


Figure 2

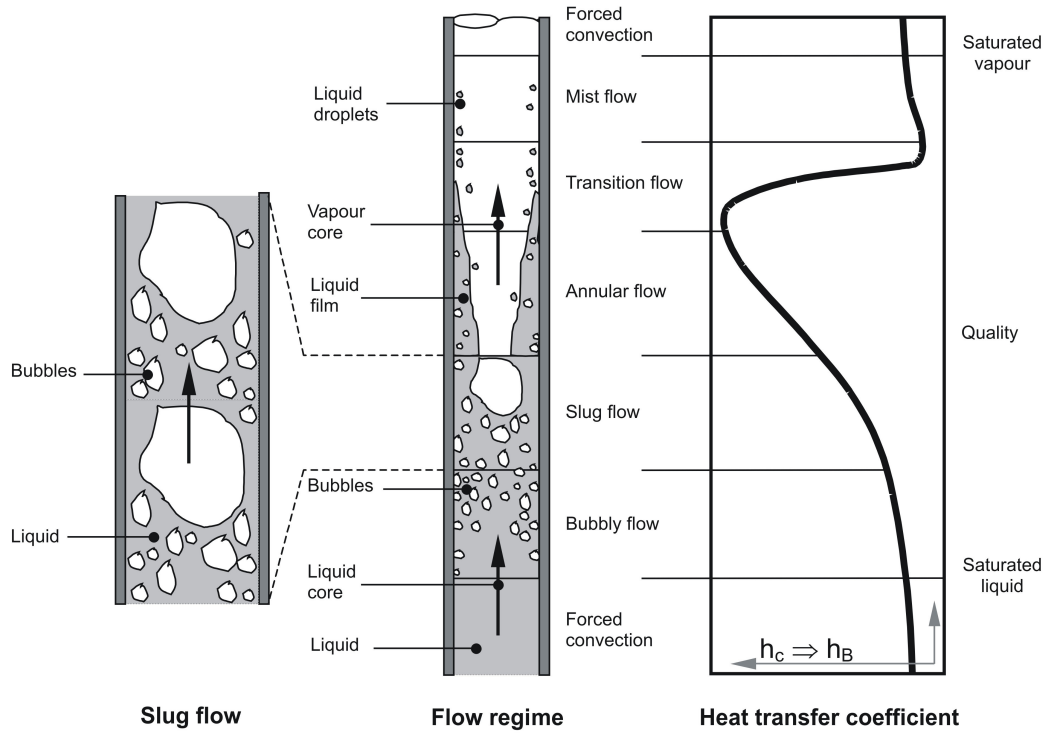
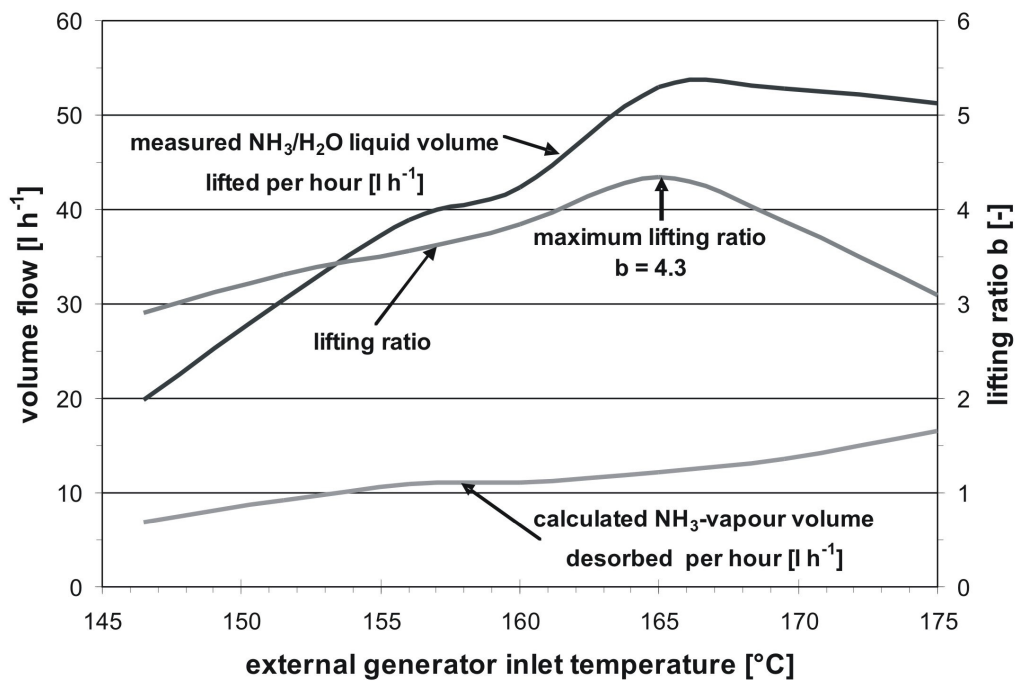


Figure 3



ACCEPTED

Figure 4

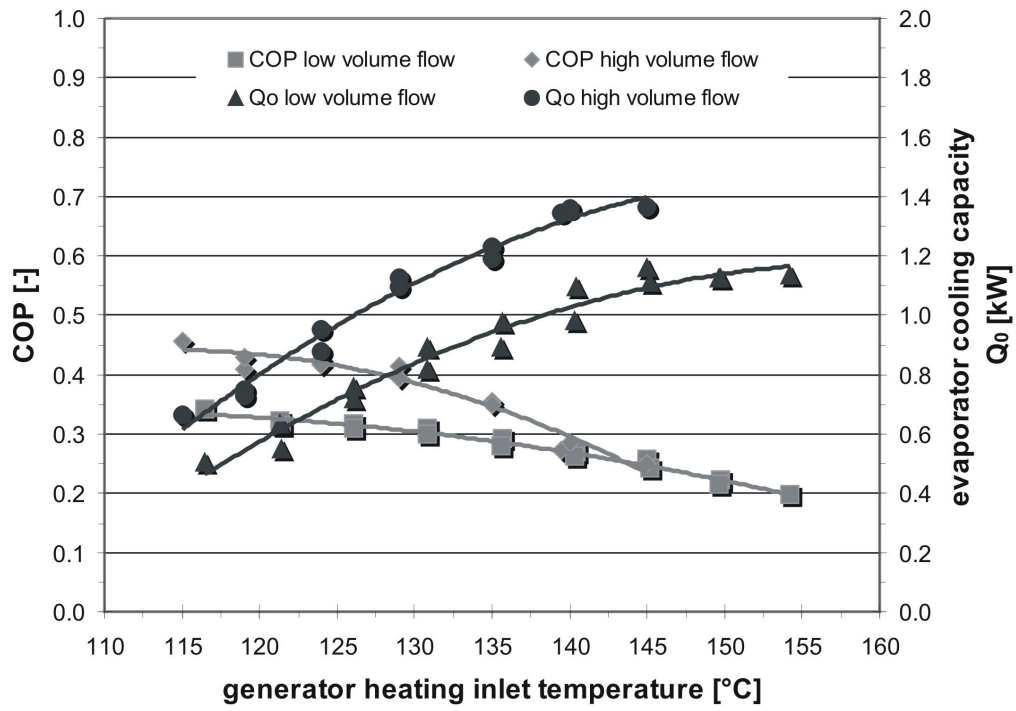


Figure 5

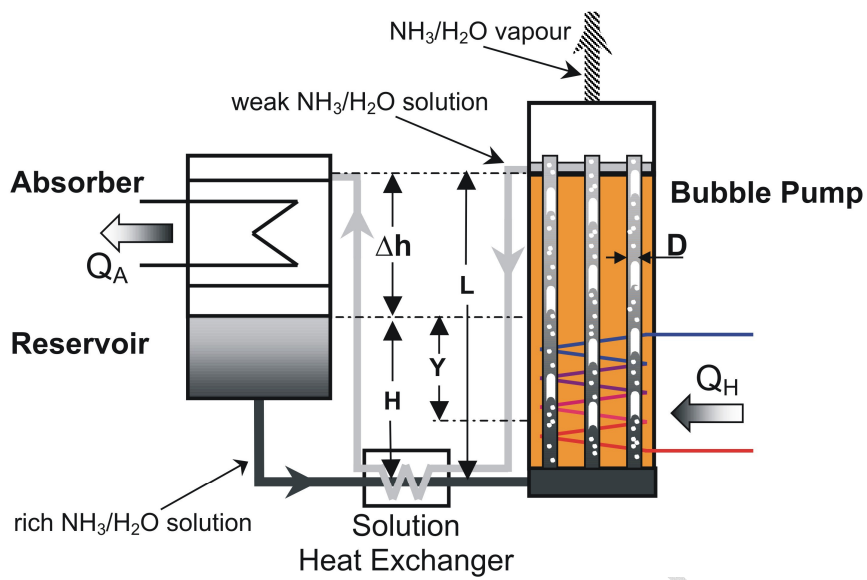
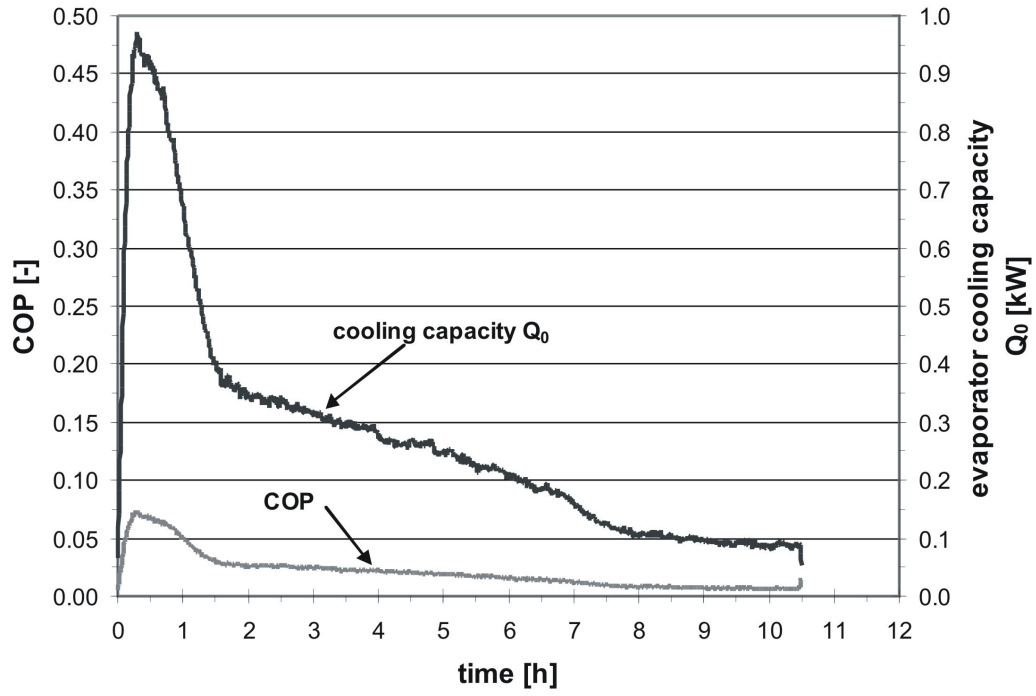
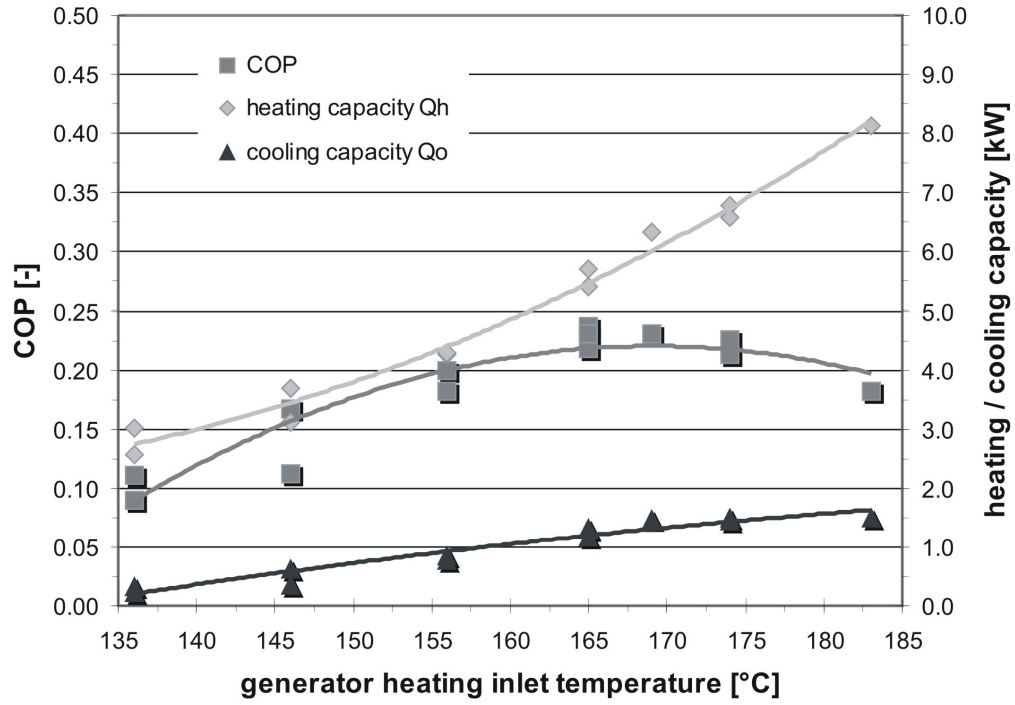


Figure 6



ACCEPTED

Figure 7



ACCEPTED

Figure 8

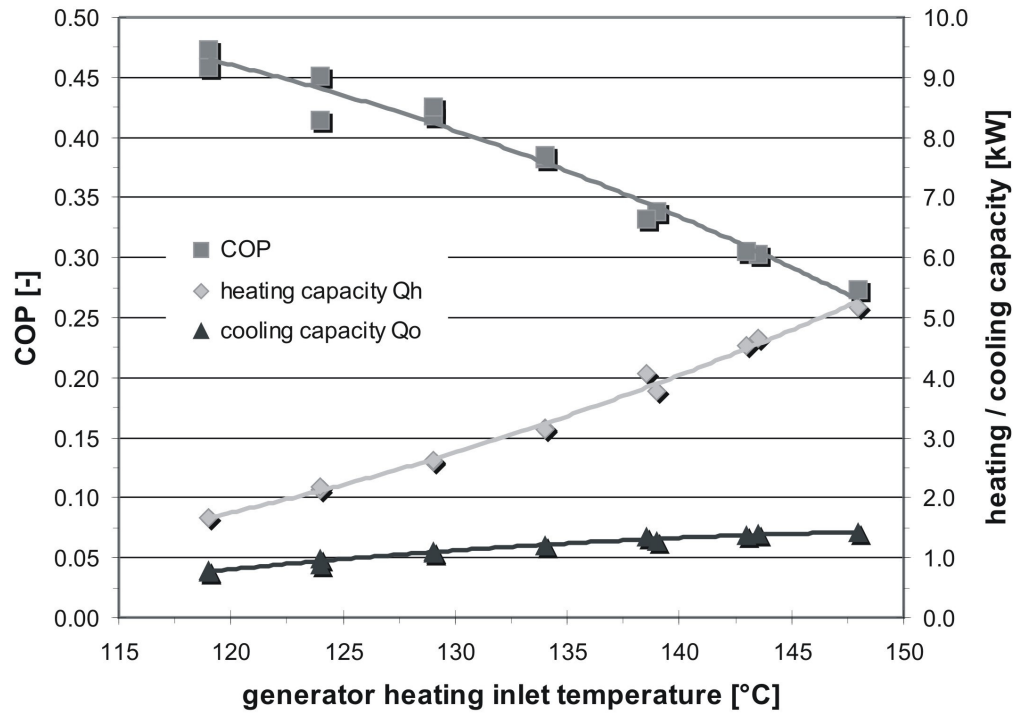


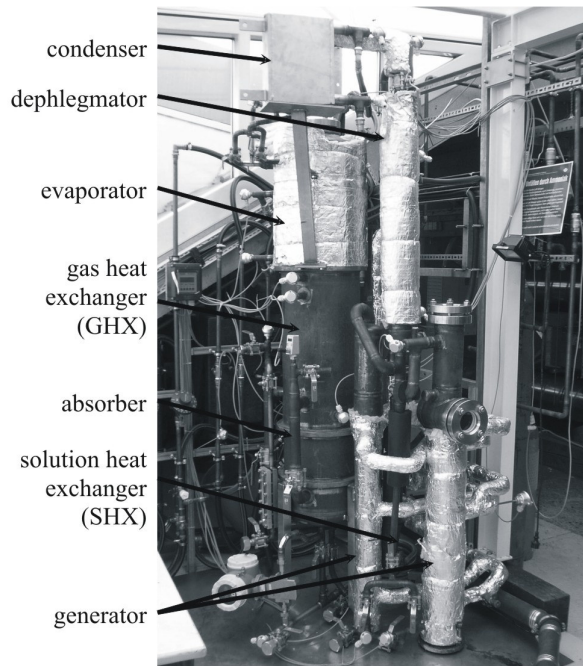
Figure 9

Figure 10

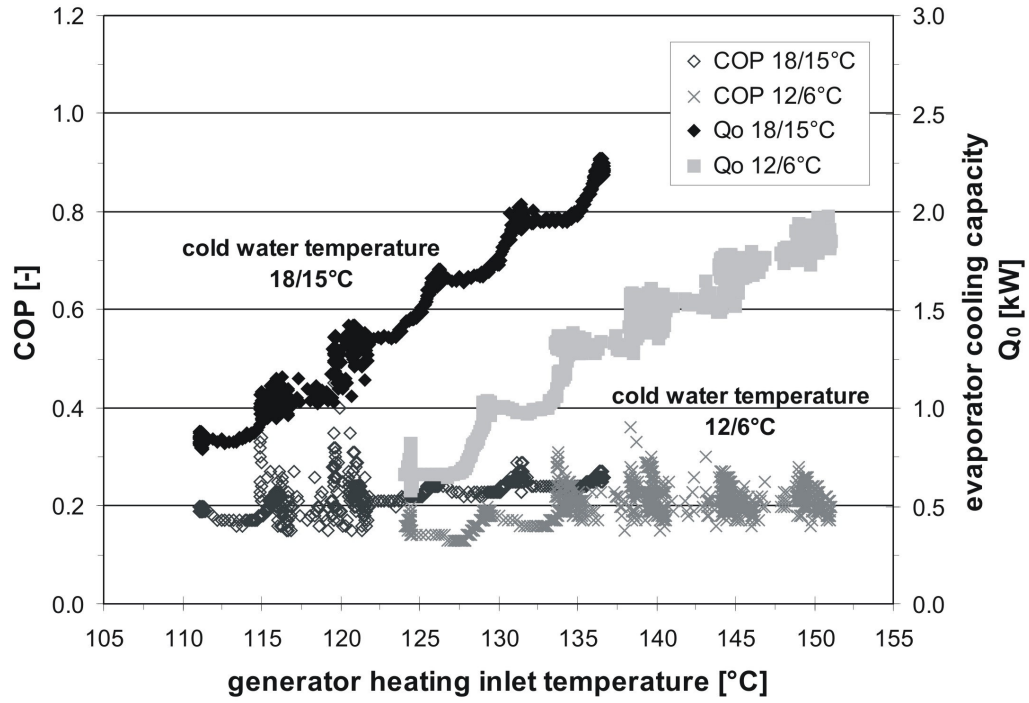


Figure 11

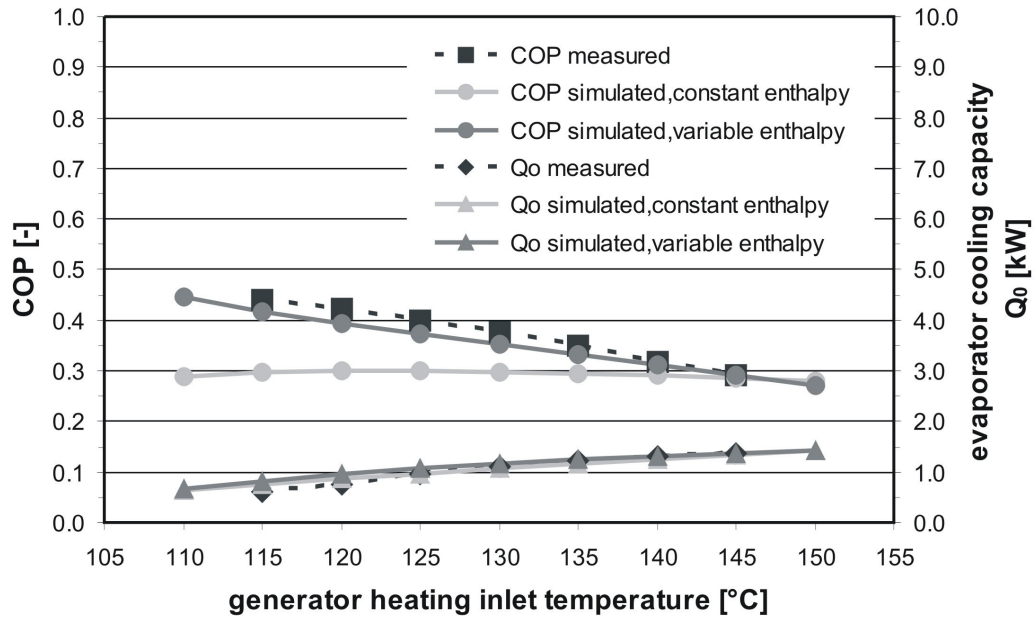
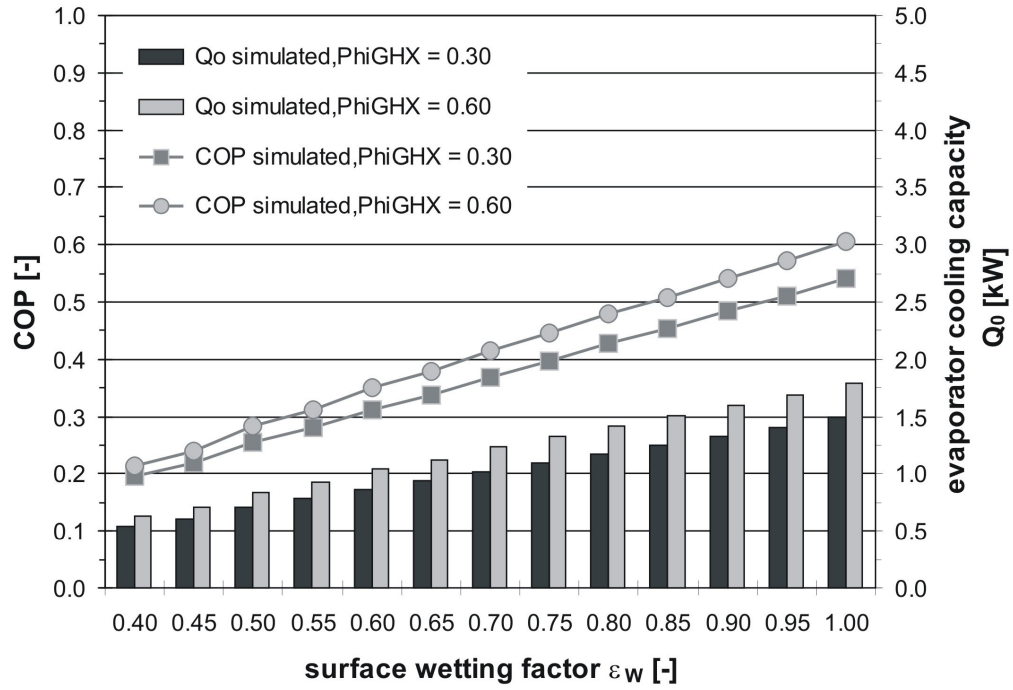


Figure 12



ACCEPTED